ARMA 12-581

AE from Undrained and Unjacketed Tests on Sandstone

Makhnenko, R.Y., Ge, C. and Labuz, J.F.
University of Minnesota, Minneapolis, MN, USA

This paper was prepared for presentation at the 46th US Rock Mechanics / Geomechanics Symposium held in Chicago, IL, USA, 24-27 June 2012.

ABSTRACT: Saturated specimens of Berea sandstone were subjected to confining pressure p and compressed axially under a plane strain condition; the biaxial deformation state is convenient for measuring axial and lateral displacements. Undrained testing involved development of pore water pressure u during application of deviatoric stress, and unjacketed tests maintained the condition of $u = p$. In addition, the specimens were instrumented with eight acoustic emission (AE) sensors for monitoring the microseismic activity during the tests.

AE events were recorded and post-processed for rate and location analyses. A significant difference was observed between unjacketed and undrained compression in terms of AE rate change with loading. For an unjacketed test, where the pore pressure inside the rock was equilibrated with the confining pressure, the number of AE events per load step remarkably increased when the axial stress reached approximately 70% of the peak, similar to the behavior of dry specimens. However, in an undrained test, where the fluid was not allowed to leave the specimen, only a few microseismic events were recorded prior to failure of the specimen. The abrupt change in the slope of the AE rate happened only when the pore pressure in the rock decreased. This effect could be explained by the delayed tendency of the rock to dilate under an undrained condition.

1. INTRODUCTION

The study of coupled effects of fluid flow and skeleton deformation in porous geomaterials is critical for proper assessment of underground structures. In fact, the presence of pore fluids can affect both the elastic parameters of the rock and the deformation process. For example, fluid in the rock may facilitate or delay material failure depending on drained or undrained response, where the local conditions will dictate the behavior [1]. Under a drained condition, the pore fluid is allowed to leave the rock and pressure is maintained at a constant level. For an undrained case, the fluid does not leave the rock so the pressure is changing. The third possible condition for fluid-rock interaction is called "unjacketed," and it is related to the case when the increase in confining pressure is equal to the increase in pore fluid pressure [2]. The influence of these conditions on behavior of porous rock is investigated by plane strain compression experiments.

Failure of rock involves the growth of microcracks from stress concentrators such as voids, inclusions, and dissimilar grain contacts. The irreversible damage results in inelastic strain and generates elastic waves known as acoustic emission (AE) [3]. The transient waves propagate through the medium with very small amplitudes and high frequencies, and the AE signals carry information about the source location and medium of propagation. The growth of damage, the onset of failure, and fracture propagation can be identified by monitoring AE [4] in dry and fluid-saturated rock specimens.

The overall project concerns the testing of water-saturated porous rock such as sandstone under plane-strain compression. Dilatant hardening and contractant softening will be investigated from drained, undrained, and unjacketed experiments, where pore pressure will be measured throughout the deformation process. This paper presents the results of unjacketed and undrained plane strain experiments. Eight acoustic emission sensors were used to monitor damage in the specimens. AE rates were compared for these two tests both in pre- and post-failure response, and locations of events were determined and compared to the global failure mechanism.

2. ACOUSTIC EMISSION

The most common acoustic emission studied in the laboratory are controlled by flaws on the scale of grain size, so that most source events are a millimeter or less in dimension. Hence, laboratory experiments are generally conducted in the 100 - 2000 kHz frequency range [3].

Two categories of laboratory AE studies are considered in this paper. The first category is a simple counting of the number of AE events prior to and after specimen failure. AE rate can then be correlated with inelastic strain rate.

The second area of research involves the location of the AE source. By recording the time histories and identifying the arrival time of the P-wave, it is possible to locate the event with an error of a few millimeters. Two assumptions are often used to simplify the problem: (i) the event is simulated as a point source of displacement discontinuity referred to as a microcrack and (ii) the elastic wave propagation is through a homogeneous, isotropic medium.

A common type of source location algorithm involves the arrival time of the P-wave. Microseismic activity due to a change in stress or environment is recorded by each sensor with a known position at a given time. From the relative arrival times of the P-wave and the measured P-wave velocity of the material, the event hypocenter can be estimated with a minimum of five sensors. The problem contains four unknowns: the spatial coordinates *x, y, z* of the event and the time at which the event occurred, but a fifth sensor (or other information) is needed to remove ambiguities arising from the quadratic nature of the distance equation. Because some error is associated with arrival-time detection (it is not always clear when a low amplitude signal arrives) and with the P-wave velocity (as damage accumulates, material properties may change or become anisotropic), the number of sensors should be increased so that the location problem becomes over-determined. Then a solution scheme can be developed whereby the error is minimized to obtain a best-fit type of solution, and statistical methods can be used to evaluate the goodness of the fit.

The distance r_i between the source and the i^{th} sensor is related to the P-wave velocity c_p by

$$r_i = c_p\left(t_i - t\right) + \varepsilon_i \qquad (1)$$

where t = time at which the event occurs, t_i = arrival time at the i^{th} sensor, and ε_i = residual of computed distances. A time shift does not affect the source location, so an arbitrary time base can be selected. The travel distance r_i can be expressed by the unknown source coordinates (x, y, z) and the known sensor coordinates (x_i, y_i, z_i) by

$$r_i = \sqrt{\left(x_i - x\right)^2 + \left(y_i - y\right)^2 + \left(z_i - z\right)^2} \qquad (2)$$

The sum of the squares of the residuals ε_i can be written

$$I = \sum_{i=1}^{N} \varepsilon_i^2 \qquad (3)$$

where N = the number of sensors. The unknowns x, y, z and t can be determined using a least-squares method by minimizing I. However, the equations are nonlinear in the source coordinates x, y, z, so the minimization is carried out numerically using the Levenberg-Marquardt algorithm. The first estimate of x, y, z is obtained by a linearization of (3).

3. EXPERIMENTAL METHODS

3.1. Plane-strain apparatus

An apparatus for determining the constitutive response of soft rock, named the University of Minnesota Plane-Strain Apparatus (Fig. 1), was designed and built based on a passive stiff-frame concept [5]. The biaxial device (U.S. Patent 5,063,785) is unique because it allows the failure plane of a specimen (1) to develop and propagate in an unrestricted manner by placing the upper platen on a low friction linear bearing (2). Plane strain deformation is enforced by a stiff biaxial frame (3), whereby the specimen is wedged against the thick-walled steel cylinder. The lateral strain can be monitored by a set of strain gages, which allows the determination of the intermediate principal stress.

Prismatic specimens of height 86 mm, thickness 44 mm, and width 100 mm are used. Applied axial load is measured by the load cells located at the bottom of the specimen (4) and on top of the pressure chamber. Five LVDTs (5) measure the displacements of the specimen and the linear bearing: two of them are attached to the upper loading platen for measuring axial displacement, a pair of LVDTs are placed horizontally on opposite sides of the specimen exposed to confining pressure for measuring lateral displacement, and one LVDT is attached to the linear bearing to record its horizontal displacement. The apparatus is placed inside a large pressure cell to induce confining (lateral) stress. The cell is filled with hydraulic oil and the confining pressure is applied with a microprocessor-based hydraulic pump that maintains cell pressure at a constant value, within a tolerance of 0.1 MPa. Up to eight AE sensors (6) can be used to monitor the microseismic activity in the specimen. In addition, the apparatus was modified to allow pore pressure to be applied and monitored both upstream and downstream (7) by two pressure transducers.

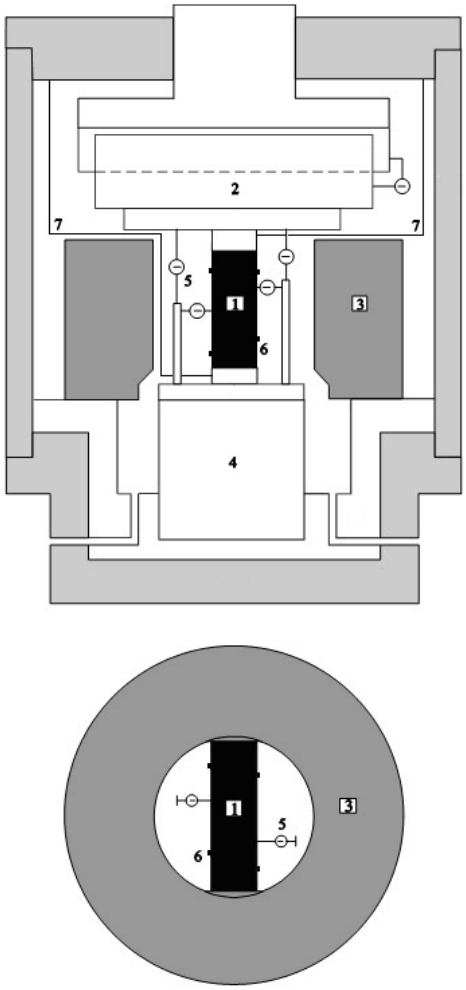

Figure 1. Sketch of the plane-strain apparatus: (1) specimen; (2) linear bearing; (3) biaxial frame; (4) load cell; (5) LVDTs; (6) AE sensors; (7) pore pressure tubes.

The specimen (Fig. 2) is assembled with porous stones between the upper and lower steel platens; the porous stones are in contact with the 100 x 44 mm faces of the specimen. Two steel plates, 3 mm thick, contact the 44 x 86 mm faces, which are covered with stearic acid to reduce the friction between the platens and the specimen. Two large (10-mm diameter) and eight small (4-mm diameter) circular brass buttons 1-mm thick are glued to the specimen to provide a firm contact for the probes of the lateral LVDTs and AE sensors. The specimen, porous stones, and platens are held together with a custom jig and a thin layer of polyurethane is applied to the 100 x 86 mm faces to prevent confining fluid from penetrating the rock.

3.2. AE system

The AE system is composed of (i) an array of AE sensors; (ii) signal conditioners and preamplifiers; (iii) signal digitizer; and (iv) computer based data acquisition system. The AE system used in this research is the same as described in [4].

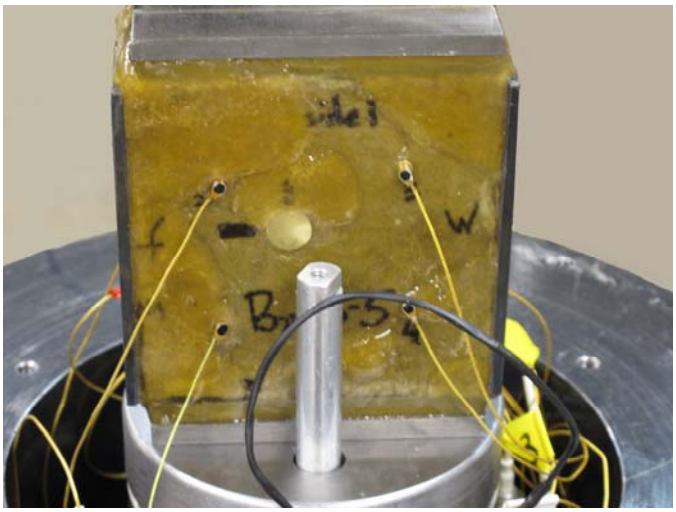

Figure 2. Specimen of Berea sandstone with AE sensors.

Eight AE sensors (Physical Acoustics model S9225) are attached with cyanoacrylate adhesive to the small brass tabs on two exposed specimen surfaces. The S9225 sensor is 3.6 mm in diameter and has a frequency response from 0.3-1.8 MHz. AE signals are preamplified with 40 dB gain and a built-in 0.1-1.2 MHz band-pass filter (Physical Acoustics S1220C). Typical noise level at the output of the preamplifiers is around ± 2 mV. The waveforms are digitized and recorded by the data acquisition system. The high-speed AE data acquisition system is composed of four modular transient recorders (LeCroy model 6840), with two channels each, 8-bit analog-to-digital (ADC) resolution and a 20 MHz sampling rate (50 nanoseconds between points) over a 100 μs window, with a 50 μs pretrigger. The LeCroy 6010 controller, with a built-in 10 MHz microprocessor (Motorola 68020), communicates to a 486-processor microcomputer through National Instrument AT-GPIB card and cable. AE data are transferred to the host computer after every 128 kbytes of digitizer memory is filled (equivalent to 64 events). The disadvantage is that there is a downloading time of approximately 4 seconds required before the system memory is ready for the next incoming AE events. All recording is triggered when the signal amplitude exceeds a certain threshold (±7 mV) on the first sensor. The threshold of amplitude must be set so that environmental noise does not trigger the system, but the threshold should not be set too high as to exclude signals of low amplitude.

3.3. Berea sandstone

The experiments were conducted on a Berea sandstone with porosity ϕ=0.23 and dry bulk density ρ=2.1 g/cm^3. The rock is flat-bedded, light gray, medium- to fine-grained protoquartzite cemented with silica and clay. Permeability of the sandstone is about 40 mD (at 5 MPa effective confining pressure), Young's modulus E=14-16

GPa, Poisson's ratio ν=0.31, uniaxial compression strength UCS=41-43 MPa.

The sandstone specimens were cut from a 300 mm side cube so that the major principal stress was applied perpendicular to bedding. All faces of the specimen were precisely ground such that opposite sides were parallel and adjacent sides were perpendicular within ±0.05 mm in 100 mm.

3.4. Test procedure

After the rock specimen is prepared and placed inside the plane-strain apparatus, it is stressed axially and laterally to 3-5 MPa, depending on desired stress state and pore pressure for the test. The next step for the undrained test is the process of water saturation, which is similar to the one described in [6]. When the equilibration of back pressure is achieved (the change of pressure does not exceed 1 kPa/min), Skempton's coefficient B is measured [7]:

$$B = \Delta u / \Delta P \tag{4}$$

where Δu is the increase in pore pressure due to the increase in mean stress ΔP.

If the system is completely saturated, the pore pressure response should be constant and independent of back pressure. On the other hand, if the system is not saturated, the pore pressure response will increase with increasing back pressure [8]. If this is the case, a new increment in back pressure is applied, and when equilibrium is reached, a new B-check is performed. When Δu becomes the same for each increment ΔP, the rock is considered to be saturated. After three days of back pressure saturation, the maximum B-value achieved for the specimen was 0.58, corrected for the compliance of the pore pressure system [8].

An unjacketed test is characterized by the equal increments of confining and pore pressure [2]. This condition is achieved by not totally covering the side faces of the specimen with polyurethane, such that confining fluid (hydraulic oil) can penetrate the specimen. Constant cell (confining) pressure during the test assures complete rock saturation.

Undrained and unjacketed deviatoric loading (compression) of the specimen is performed on the saturated specimens. An average lateral displacement rate of 0.03 micron/s is used as the feedback signal within the closed-loop, servo-hydraulic testing system. It is assumed that this rate is slow enough to ensure an even distribution of pore fluid pressure in the specimens. The average lateral displacement is used as the feedback signal to the servo-controller. This choice results in an imposed axial strain rate that is decreasing close to the peak axial stress. The tests are stopped when the residual strength is reached.

4. EXPERIMENTAL RESULTS

4.1. AE locations

Acoustic emission locations were determined for specimens tested under unjacketed and dry conditions. For accurate determination of AE locations, P-wave velocity is measured at different effective stresses. For the tests described, c_p at 5 MPa confining pressure is 2700 m/s, while c_p=3200 m/s at 5 MPa confining pressure and pore pressure (zero effective confining pressure) for the unjacketed test; c_p=2100 m/s for a dry specimen at atmospheric pressure. Time of first arrival information is extracted from the P-waves using an algorithm described in [9].

Processing of the AE data recorded for the dry test provided 1834 locations with error less than 3 mm, out of 9254 total events. Before the peak load was reached, AE events were scattered in the specimen (Fig. 3a). However, in the post-peak region, located events closely follow the failure mechanism (Fig. 3b, 3c), which in this test is an inclined fracture (Fig. 3d).

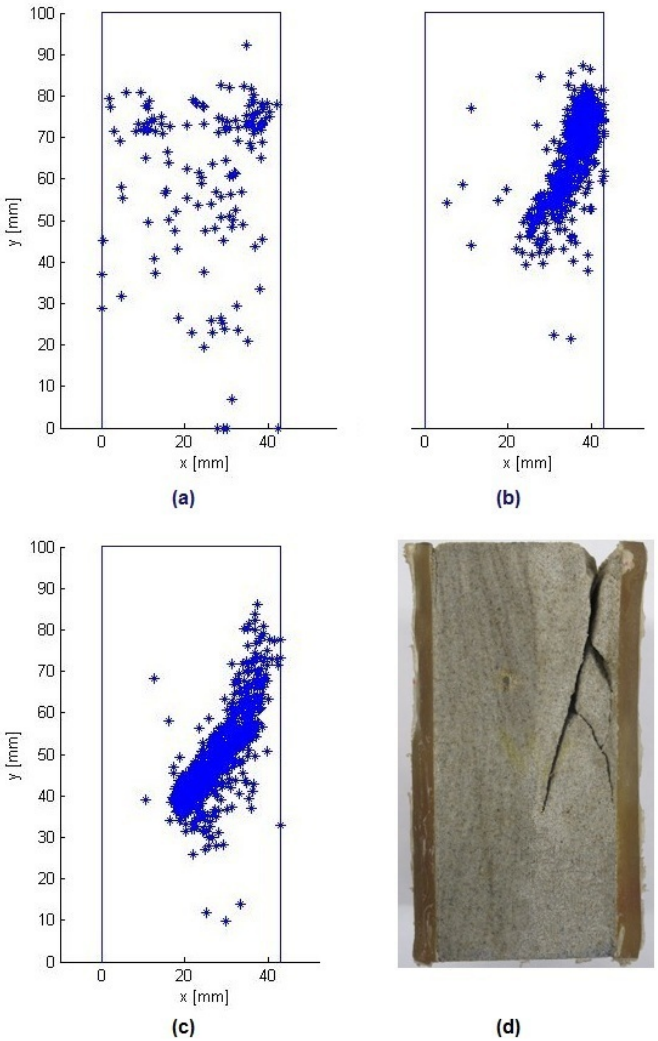

Figure 3. Drained test (dry specimen). Projection of AE events location (a) pre-peak, (b) peak - 90% post-peak, (c) 90% post-peak - residual; (d) photo of failed specimen.

Locations of AE for the unjacketed test (Fig. 4a) also follow the failure mechanism (Fig. 4b). The effective confinement for unjacketed test is zero, so it is natural that the observed failure type is close to axial splitting.

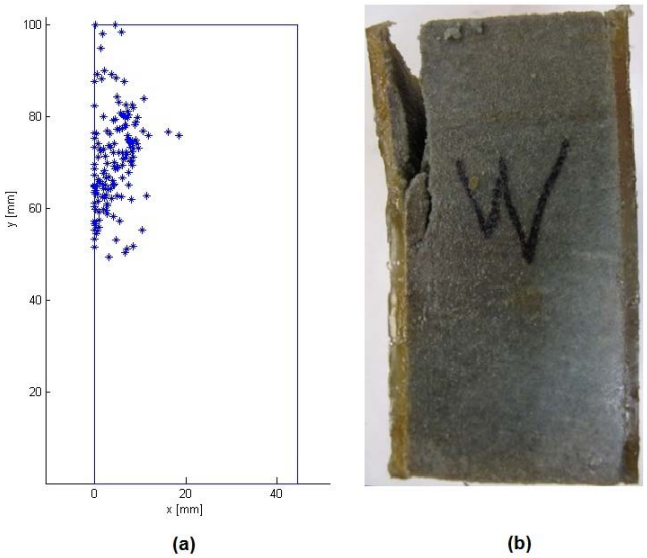

Figure 4. Unjacketed test. (a) Projection of AE events location; (b) photo of failed specimen.

4.2. AE rate

The rates of acoustic emission events are presented on the following figures with the axial load and volumetric strain data for the unjacketed test (Figs. 5a and 5b respectively) and with the load and pore pressure data for the undrained test (Figs. 6a and 6b).

A significant difference was observed between the unjacketed and undrained plane strain compression tests in relation to the AE. For the unjacketed test, where the pore pressure inside the rock is equilibrated with the confining pressure, the number of AE events per minute remarkably increased (from 6 events/min to 55 events/min) when the axial load on the specimen reached approximately 70% of peak load (Fig. 5a), which is also the case for plane strain experiments performed with the same rock tested dry [10]. It can be seen in Figs. 5a and 5b that the abrupt change in AE rate (marked with the dashed line) happens approximately when the load-displacement curve deviates from linear behavior, and volumetric strain starts decreasing; for the sign convention of compression positive, "decrease" means dilation. Thus, the onset of inelastic deformation in the form of dilatant behavior is associated with an increase in AE rate.

In an undrained test, an approximately constant AE rate of 3 events/min was recorded prior to peak axial stress (Fig. 6a). The slope of the AE curve abruptly increased to 210 events/min only at the peak load, which is indicated by the dashed line. The AE rate was approximately constant in the post peak region before the residual strength was reached. The significant change in AE activity approximately coincided with drop of the pore pressure in the rock (Fig. 6b), which happens due to localization of deformation and appearance of a fracture. The observed effect could be explained by the delayed tendency to dilate for the rock under an undrained condition and the fact that an increase in specimen volume is usually accompanied by intense microcracking, where the AE rate should be increasing.

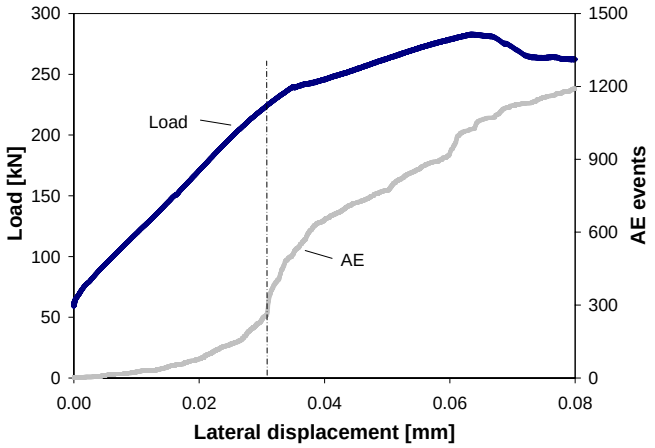

Figure 5a. Mechanical response and AE for unjacketed test.

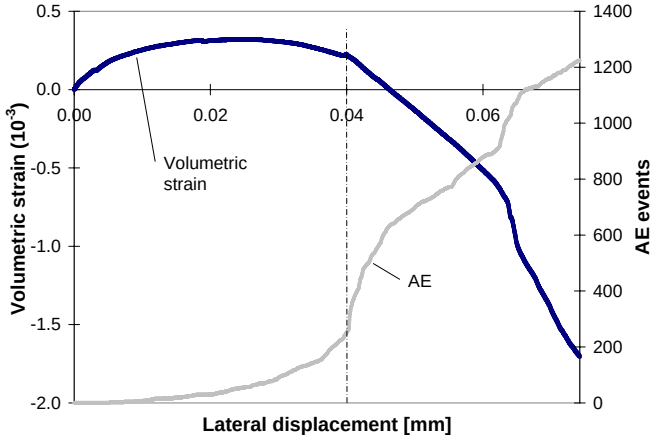

Figure 5b. Volumetric strain and AE for unjacketed test.

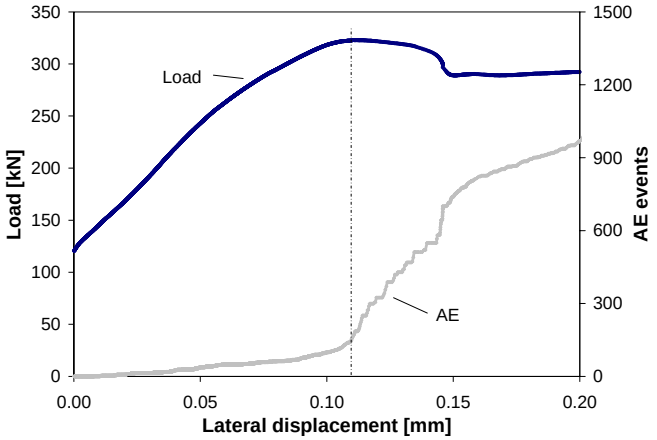

Figure 6a. Mechanical response and AE for undrained test.

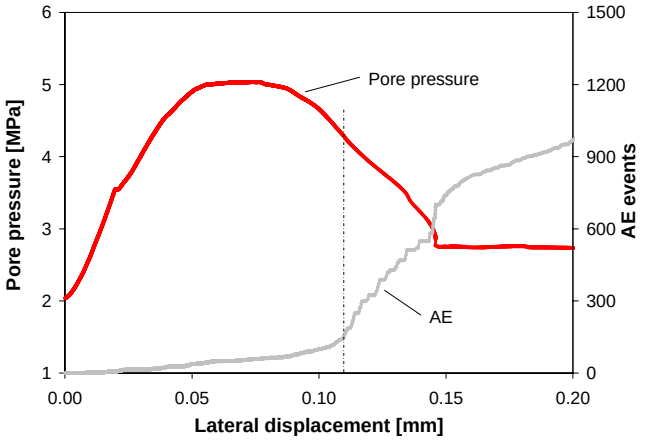

Figure 6b. Pore pressure and AE for undrained test.

5. CONCLUDING REMARKS

Berea sandstone was tested under undrained and unjacketed conditions within the University of Minnesota Plane-Strain Apparatus. Locations of acoustic emission (AE) events can be precisely determined before and after failure in dry and fluid-saturated rock specimens. AE rates were found to be different under unjacketed and undrained conditions. In an unjacketed test, the AE behavior was similar to that one for a drained test (dry specimen), *i.e.* the AE rate significantly increased at the onset of inelastic deformation. However, when the rock was tested under an undrained condition, intensive microcracking was observed only when the peak axial stress was reached and when the material exhibited a tendency to dilate.

ACKNOWLEDGEMENTS: Partial support was provided by DOE Grant DE-FE0002020 funded through the American Recovery and Reinvestment Act.

REFERENCES

1. Rice, J.R. 1975. On the stability of dilatant hardening for saturated rock masses. *J. Geophys. Res.* 80(11): 1531-1536.
2. Detournay, E. and A. Cheng. 1993. Fundamentals of poroelasticity. In *Comprehensive Rock Engineering, Vol. II*, ed. C. Fairhurst, 113-171.
3. Lockner, D. 1993. The role of acoustic emission in the study of rock fracture. *Int. J. Rock Mech. Min. Sci. & Geomech. Abstr.* 30(7): 883-899.
4. Dai, S.T. and J.F. Labuz. 1997. Damage and failure analysis of brittle materials by acoustic emission. *J. Materials in Civ. Eng.* 9(4): 200-205.
5. Labuz, J.F., S.T. Dai, and E. Papamichos. 1996. Plane-strain compression of rock-like materials. *Int. J. Rock Mech. Min. Sci.* 33(6): 573-584.
6. Makhnenko, R.Y., J.J. Riedel, and J.F. Labuz. 2011. Undrained plane strain compression of shale. In *Proceedings of 45th US Rock Mechanics/ Geomechanics Symposium, San Francisco, 26-29 June 2011.*
7. Bishop, A.W. 1973. The influence of an undrained change in stress on the pore-pressure in porous media of low compressibility. *Geotechnique*. 23(3): 435-442.
8. Wissa, A.E. 1969. Pore pressure measurements in saturated stiff soils. *J. Soil Mech. & Found. Division, ASCE*. 95: 1063-1073.
9. Ince, N.F., C.-S. Kao, M. Kaveh, A. Tewfik, and J.F. Labuz. 2009. Averaged acoustic emission events for accurate damage localization. In *Proceedings of IEEE International Conference on Acoustics, Speech and Signal Processing, 2009.*
10. Riedel, J.J. and J.F. Labuz. 2007. Propagation of a shear band in sandstone. *Int J. Num. Anal. Meth. Geomech.* 31: 1281-1299.